

Spring 5-2017

## **Altering the Structure of Carboxysomal Carbonic Anhydrase CsoSCA to Determine the Necessity of the N-terminal Domain in CsoSCA Function**

Dana L. Dillistone  
*University of Southern Mississippi*

Follow this and additional works at: [https://aquila.usm.edu/honors\\_theses](https://aquila.usm.edu/honors_theses)



Part of the [Biochemistry Commons](#)

---

### **Recommended Citation**

Dillistone, Dana L., "Altering the Structure of Carboxysomal Carbonic Anhydrase CsoSCA to Determine the Necessity of the N-terminal Domain in CsoSCA Function" (2017). *Honors Theses*. 520.  
[https://aquila.usm.edu/honors\\_theses/520](https://aquila.usm.edu/honors_theses/520)

This Honors College Thesis is brought to you for free and open access by the Honors College at The Aquila Digital Community. It has been accepted for inclusion in Honors Theses by an authorized administrator of The Aquila Digital Community. For more information, please contact [Joshua.Cromwell@usm.edu](mailto:Joshua.Cromwell@usm.edu), [Jennie.Vance@usm.edu](mailto:Jennie.Vance@usm.edu).

The University of Southern Mississippi

Altering the Structure of Carboxysomal Carbonic Anhydrase CsoSCA to Determine the  
Necessity of the N-terminal Domain in CsoSCA Function

by

Dana Dillistone

A Thesis  
Submitted to the Honors College of  
The University of Southern Mississippi  
In Partial Fulfillment  
Of the Requirements for the Degree of  
Bachelor of Science  
In the Department of Chemistry and Biochemistry

May 2017

Approved by

---

Sabine Heinhorst, Ph.D., Thesis Adviser  
Professor of Biochemistry

---

Sabine Heinhorst, Ph.D., Chair  
Department of Chemistry and  
Biochemistry

---

Ellen Weinauer, Ph.D., Dean  
Honors College

## Abstract

In this project, a DNA construct was designed and developed to remove the first fifty amino acids of the CsoSCA protein in the chemolithotrophic bacterium *Halothiobacillus neapolitanus*. The *csoS3* gene codes for a carbonic anhydrase enzyme (CsoSCA) that is unique to a structure called a carboxysome. Carboxysomes are polyhedral microcompartments where carbon fixation is housed. The carbonic anhydrase is a shell-associated protein that improves the catalytic efficiency of ribulose-bisphosphate carboxylase/oxygenase (RuBisCO), the enzyme that catalyzes the fixation of carbon. By deleting the first fifty amino acids of the carbonic anhydrase, the necessity of the amino acids in carboxysome function was evaluated.

The construct was designed by removing 150 bases from the coding sequence and by adding a kanamycin resistance cassette for selection of recombinant colonies. Regions of homology to the *csoS2* and *csoS3* coding regions were included for homologous recombination in *E. coli* DY330. Once the recombination event was successful, the isolated DNA was used for gene replacement in *H. neapolitanus*. Growth curves were generated for *H. neapolitanus* wildtype, a mutant in which *csoS3* was deleted entirely, and the mutant generated with the designed construct (truncated *csoS3*). Comparing the growth curves of the wildtype and the mutants, it was found that while the mutant carrying the truncated carbonic anhydrase gene did not grow in air as well as wildtype, it grew considerably better than the deletion mutant. Deleting the codons for the first fifty amino acids of *csoS3* does affect carboxysome function, but not as much as complete *csoS3* deletion.

Keywords: carboxysome, homologous recombination, carbonic anhydrase, *csoS3*,  
CsoSCA, *Halothiobacillus neapolitanus*

## **Acknowledgements**

I would like to acknowledge Dr. Heinhorst, my thesis advisor, for being gracious and patient with me while still pushing me to be the best student I could be. Thank you for always being understanding and meeting with me when I had questions. Without your guidance, I would have been utterly lost. I am so appreciative that you allowed me to complete my research under you and that you spent so much time investing in me and teaching me. You have taught me more than you know.

I would also like to acknowledge Daniela del Valle for guiding me in the laboratory. Thank you for training me in lab techniques and being kind yet direct when I made mistakes. I am thankful for your patience when I worked slowly as I was learning. Thank you for always answering my endless questions (and making me figure out most of them on my own). Thank you for making the lab a pleasant place to work.

Finally, I would like to acknowledge the Honors College and the Department of Chemistry and Biochemistry for not only challenging me to be a hard-working student but also encouraging me to excel in all areas of life. I feel equipped to enter the next chapter as a more knowledgeable, well-rounded individual. Thank you for supporting my undergraduate career.

## Table of Contents

<b>List of Tables.....</b>	<b>vii</b>
<b>List of Figures.....</b>	<b>viii</b>
<b>Chapter I: Introduction.....</b>	<b>1</b>
<b>Chapter 2: Literature Review.....</b>	<b>3</b>
<b>Chapter III: Materials and Methods.....</b>	<b>10</b>
Overlap Extension Polymerase Chain Reaction.....	13
Cloning and Recombination in <i>E. coli</i> DY330.....	17
Gene Replacement in <i>H. neapolitanus</i> .....	21
Growth curves.....	22
<b>Chapter IV: Results.....</b>	<b>22</b>
Overlap Extension Polymerase Chain Reaction.....	24
Cloning and Recombination in <i>E. coli</i> DY330.....	30
Gene Replacement in <i>H. neapolitanus</i> .....	34
Growth curves.....	37
<b>Chapter V: Discussion and Conclusion.....</b>	<b>41</b>
<b>Literature Cited.....</b>	<b>43</b>

## List of Tables

<b>Table 1:</b> PCR 1 and PCR 2 Reaction Mixtures.....	14
<b>Table 2:</b> PCR 1 Parameters.....	14
<b>Table 3:</b> PCR 2 Parameters.....	15
<b>Table 4:</b> PCR 3 Reaction Mixtures.....	16
<b>Table 5:</b> PCR 3 Parameters.....	16
<b>Table 6:</b> PCR Screening Parameters.....	19
<b>Table 7:</b> Enzyme Restriction Reaction.....	20
<b>Table 8:</b> Overlap Extension PCR Temperature Gradient (°C) .....	29
<b>Table 9:</b> Growth Curves for Wild Type, <i>csoS3</i> Deletion Mutant, and <i>csoS3</i> Truncated Mutant in Air.....	38
<b>Table 10:</b> Growth Curves for Wild Type, <i>csoS3</i> Deletion Mutant, and <i>csoS3</i> Truncated Mutant in CO <sub>2</sub> .....	39

## List of Figures

<b>Figure 1:</b> Calvin-Benson-Bassham Cycle.....	3
<b>Figure 2:</b> (A) Transmission electron micrograph of <i>H. neapolitanus</i> cell (B) Purified intact carboxysomes (negatively stained) (C) Carboxysomes after rupture (negatively stained) .....	5
<b>Figure 3:</b> The CO <sub>2</sub> concentrating mechanism of autotrophic bacteria.....	6
<b>Figure 4:</b> <i>H. neapolitanus</i> <i>cso</i> operon.....	7
<b>Figure 5:</b> Stereo view of CsoSCA highlighting its three domains.....	8
<b>Figure 6:</b> Construct Design.....	23
<b>Figure 7:</b> Flow Chart.....	24
<b>Figure 8:</b> Primer Design for PCR 1.....	25
<b>Figure 9:</b> Primer Design for PCR 2.....	26
<b>Figure 10:</b> Primer Design for PCR 3.....	27
<b>Figure 11:</b> Analytical Gel Electrophoresis of PCR Products.....	28
<b>Figure 12:</b> Analytical Gel Electrophoresis of the Overlap Extension PCR.....	29
<b>Figure 13:</b> Preparative Gel Electrophoresis of Reactions 3 and 4 of the Overlap Extension PCR.....	30
<b>Figure 14:</b> Homologous Recombination.....	31
<b>Figure 15:</b> PCR Screening of <i>E. coli</i> Top-10 Transformants.....	32
<b>Figure 16:</b> Linear Donor Fragment after Amplification by PCR.....	33
<b>Figure 17:</b> PCR Screening of Transformant Colonies.....	34
<b>Figure 18:</b> Preparative Gel Electrophoresis of Enzyme Digest for Ligation Reaction.....	35
<b>Figure 19:</b> Analytical Gel Electrophoresis of <i>E. coli</i> Top 10 Transformants.....	36
<b>Figure 20:</b> Analytical Gel Electrophoresis of PCR Screening of <i>H.nea</i> Mutants 4 and 5.....	37
<b>Figure 21:</b> Growth Curve Values for Wild Type, <i>csoS3</i> Deletion Mutant, and <i>csoS3</i> Truncated Mutant in Air.....	39
<b>Figure 22:</b> Growth Curve Values for Wild Type, <i>csoS3</i> Deletion Mutant, and <i>csoS3</i> Truncated Mutant in CO <sub>2</sub> .....	40

## ***Chapter I: Introduction***

Cyanobacteria and many chemolithotrophic bacteria contain polyhedral microcompartments called carboxysomes<sup>1</sup>. *Halothiobacillus neapolitanus*, a sulfur oxidizing chemolithotroph, is one such microorganism that contains this type of microcompartment and is the model organism in studies involving carboxysomes. Carboxysomes contain the enzyme ribulose-bisphosphate carboxylase/oxygenase (RuBisCO), which catalyzes carbon fixation, a process that converts carbon dioxide to organic compounds needed by the bacteria<sup>1</sup>. The carboxysome also contains the shell protein CsoSCA, which is a carbonic anhydrase<sup>1</sup>. The role of carbonic anhydrase is to equilibrate  $\text{HCO}_3^-$  and  $\text{CO}_2$ , which supplies RuBisCO with its substrate,  $\text{CO}_2$ <sup>2</sup>. Once  $\text{HCO}_3^-$  is converted to  $\text{CO}_2$ , the protein shell is thought to act as a “carbon dioxide trap,” meaning that the diffusion of carbon dioxide out of the microcompartment is limited<sup>1</sup>. The carbon dioxide, then, is more accessible to RuBisCO. This improves catalytic efficiency of RuBisCO, therefore increasing the rate at which carbon fixation occurs.

CsoSCA dehydrates bicarbonate through a time efficient equilibration to generate carbon dioxide. CsoSCA is found in the shell in low abundance, which indicates that it is not likely crucial for assembly of the carboxysome shell structure; however, it is necessary for carboxysome function<sup>3</sup>. CsoSCA in *H. neapolitanus* and related bacteria is a  $\beta$ -type carbonic anhydrase with three domains: an N-terminal domain, the catalytic domain, and a C-terminal domain<sup>3</sup>. When compared to other carbonic anhydrases of the  $\beta$ -class, the catalytic domain of CsoSCA from *H. neapolitanus* strongly resembles them<sup>3</sup>. The C-terminal domain is somewhat similar to the catalytic domain<sup>3</sup>. The N-terminal domain, however, is structurally different from other  $\beta$ -type carbonic anhydrases<sup>3</sup>.

The N-terminal domain of CsoSCA is made up of residues 1-144 and is formed mainly by four  $\alpha$ -helices<sup>3</sup>. When analyzing the structure of the carboxysomal  $\beta$ -carbonic anhydrase, Sawaya *et al.* noticed that the N-terminal domain was at a secluded end of the protein and noted that this could mean that its role is to secure CsoSCA to the shell of the carboxysome or to RuBisCO<sup>3</sup>. Because the structure of the N-terminal domain is unique and the function of this part of the protein is not understood, the proposed project will focus on this domain. By altering CsoSCA through removal of the N-terminal domain, this study will assess the necessity of this domain for incorporation into the carboxysome and in the catalytic function of CsoSCA.

## Chapter II: Literature Review

Chemolithotrophic bacteria use inorganic chemicals as electron donors and sources of energy. Sulfur oxidizing bacteria, a specific group of chemolithotrophic bacteria, oxidize sulfides, sulfur, and thiosulfate to produce sulfuric acid<sup>4</sup>. The electrons and ATP produced during the oxidation of these inorganic sulfur-containing compounds are used by chemolithotrophs in autotrophy to reduce carbon dioxide to usable organic compounds. This process is known as chemosynthesis, which is inorganic carbon fixation aided by the oxidation of inorganic material. Sulfur oxidizing bacteria use the Calvin-Benson-Bassham cycle (**Figure 1**) to accomplish chemosynthesis.

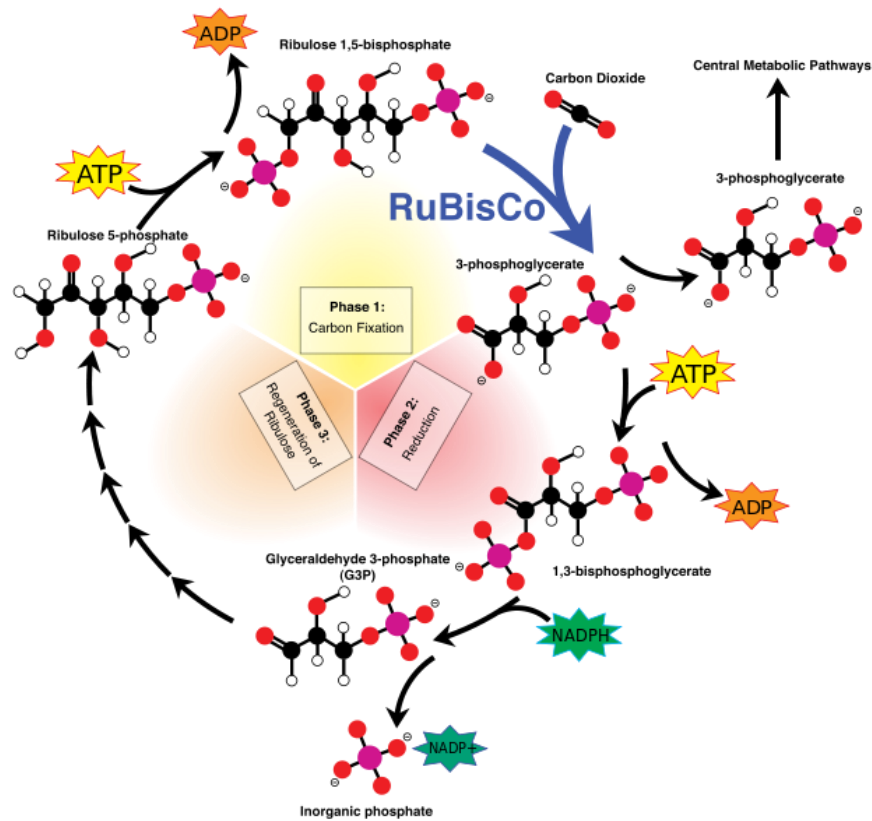


**Figure 1.** Calvin-Benson-Bassham Cycle. Carbon fixation occurs in the first phase of the cycle. Retrieved and reprinted from <http://chemwiki.ucdavis.edu>

Carbon fixation occurs in the first step of the cycle. In this step, the enzyme ribulose 1,5-bisphosphate carboxylase/oxygenase, referred to as RuBisCO, acts as a catalyst for the carboxylation of ribulose-1,5-bisphosphate (RuBP) with carbon dioxide through a two-step reaction. The product is an unstable six-carbon intermediate compound. This intermediate is then hydrolyzed to produce two molecules of 3-phosphoglycerate. These molecules can be reduced in the next step in order to make sugars as illustrated in **Figure 1**. The carbon dioxide is used to generate the carbon skeleton of the sugars. The acceptor of carbon dioxide is regenerated in the cycle.

Cyanobacteria and many chemolithotrophic bacteria fix carbon in polyhedral microcompartments called carboxysomes. Carboxysomes consist of protein shells that encapsulate the RuBisCO enzyme that catalyzes carbon fixation<sup>5</sup>. The first carboxysomes that were purified and analyzed were the carboxysomes of the bacterium *Halothiobacillus neapolitanus*<sup>6</sup>, and this bacterium is still the model organism for their study. *H. neapolitanus* is a sulfur-oxidizing chemolithotroph that utilizes thiosulfate as its energy and electron source. In **Figure 2A**, an electron micrograph of these microcompartments in a *H. neapolitanus* cell is shown.

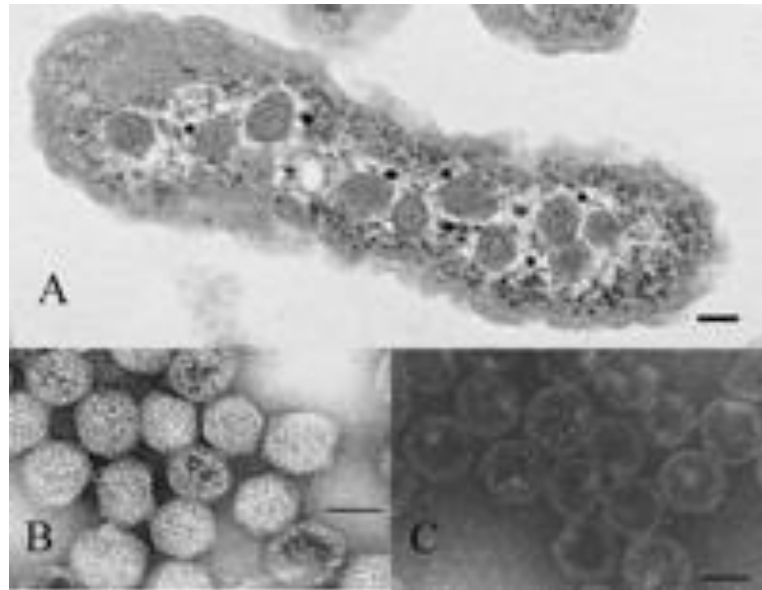


**Figure 2.** (A) Transmission electro micrograph of *H. neapolitanus* cell (B) Purified intact carboxysomes (negatively stained) (C) Carboxysomes after rupture (negatively stained). Heinhorst et al. 2006. J. Bacteriol. 188: 8087-8094.

The carboxysome enhances the efficiency of carbon fixation. Although RuBisCO is a critical component of the Calvin-Benson-Bassham cycle, it is not an efficient catalyst. RuBisCO has a low affinity for CO<sub>2</sub>, a low turnover number, and does not discriminate between CO<sub>2</sub> and O<sub>2</sub> (the competing substrate for the enzyme) very well<sup>2</sup>. Bacteria that contain carboxysomes reside in areas in which the concentration of CO<sub>2</sub> is less than the K<sub>m</sub> of RuBisCO<sup>2</sup>. The CO<sub>2</sub> concentrating mechanism (CCM) of autotrophic bacteria shown in **Figure 3** demonstrates how the weak points of RuBisCO are overcome. Through the CCM, the bicarbonate that accumulates in the cell is efficiently converted to the substrate of RubisCO by the carbonic anhydrase. The low CO<sub>2</sub> permeability of the carboxysome shell then traps the RubisCO substrate inside the carboxysome.

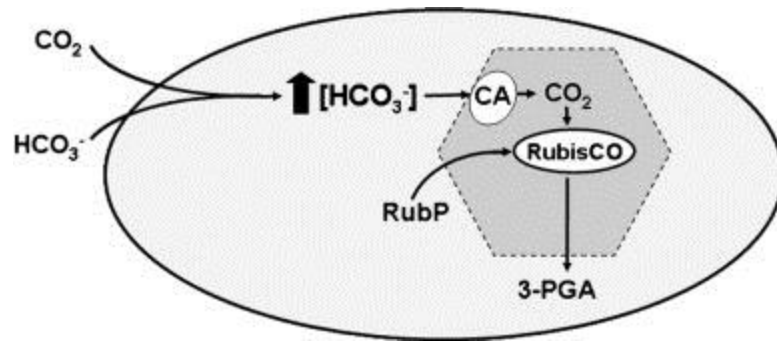


**Figure 3.** The CO<sub>2</sub> concentrating mechanism of autotrophic bacteria. Cannon, Heinhorst and Kerfeld. 2010. BBA – Proteins and Proteomics, 1804(2): 382-392.

Carbon dioxide and bicarbonate enter the intracellular space through a transporter.

Carbon dioxide and bicarbonate exist in equilibrium in the intracellular space shown in the following equation:



When applying Le Châtelier's principle to equation 1, it can be seen that the slightly basic pH (~7.4) of the intracellular space causes the equilibrium to lie in favor of bicarbonate<sup>2</sup>. Because bicarbonate is a charged moiety, it cannot escape through the phospholipid bilayer and remains in high concentrations in the cell. In addition to RuBisCO, the carboxysome contains another enzyme known as carbonic anhydrase or CsoSCA (formerly CsoS3 after the *csoS3* gene that codes for the protein)<sup>3</sup>. The carbonic anhydrase quickly dehydrates the captured bicarbonate to carbon dioxide, RuBisCO's substrate. Once RuBisCO has access to its substrate, carbon fixation can occur. Carbonic anhydrase increases the catalytic efficiency of RuBisCO and therefore increases the overall rate of carbon fixation. Additionally, proteins that are abundant shell proteins are thought to limit the diffusion of carbon dioxide out of the carboxysome<sup>7</sup>. This reduced permeability of the carboxysome shell for carbon dioxide further increases catalytic

efficiency by ensuring that RuBisCO can access sufficient CO<sub>2</sub> in the carboxysome interior.

The carbonic anhydrase is a carboxysomal protein that is tightly associated with the carboxysome shell<sup>2</sup> and is critical for the function of the carboxysome<sup>7</sup>. This protein is present in low abundance in the carboxysome, representing only about 8% of the total shell protein<sup>1</sup>. CsoSCA was shown to be a novel carbonic anhydrase unique to  $\alpha$ -carboxysomes and was renamed CsoSCA to indicate its shell association. The *cso* operon of *H. neapolitanus* is shown in **Figure 4**.

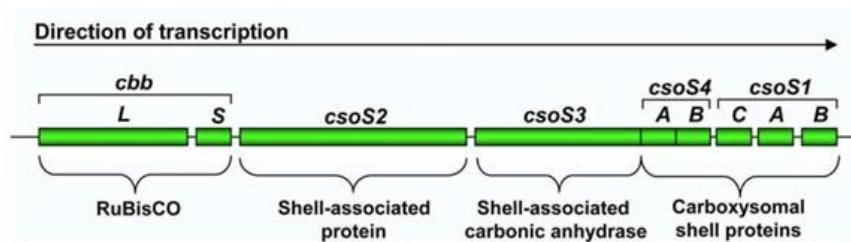


**Figure 4.** *H. neapolitanus* *cso* operon. Menon et al. 2008. Plos ONE, 3(10): 1-10.

This operon contains the genes for Form I RuBisCO (*cbbL* and *cbbS*) and for the carboxysomal shell proteins (*csoS2*, *csoS3*, *csoS4A*, *csoS4B*, *csoS1C*, *csoS1A*, and *csoS1B*). The gene on which this study is focused is *csoS3*, the gene encoding the shell-associated carbonic anhydrase CsoSCA.

CsoSCA is composed of three domains: an N-terminal domain (residues 38-144), a catalytic domain (residues 151-397), and a C-terminal domain (residues 398-514)<sup>3</sup>. These domains can be seen in **Figure 5**. Residues 1-37 (N-terminal residues) and 145-150 (residues connecting the N-terminal and catalytic domains) are not included in the structural model; the crystallographers assume this is because of disorder in these regions.

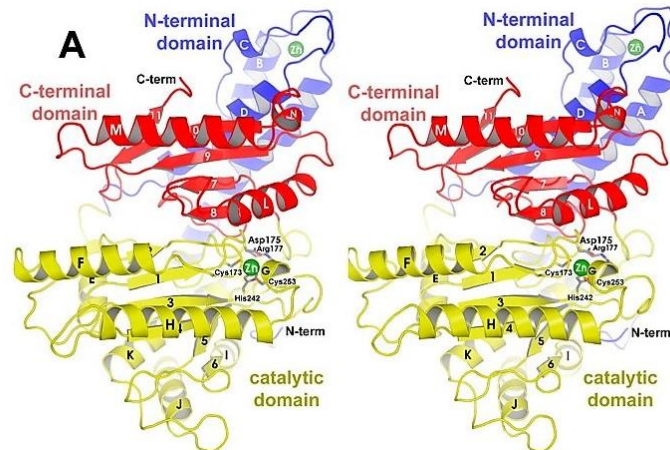


**Figure 5.** Stereo view of CsoSCA highlighting its three domains. Sawaya et al. 2006. *J Biol Chem*, 281: 7546–7555.

While the catalytic and C-terminal domains are similar to those found in other  $\beta$ -type carbonic anhydrases, the N-terminal domain is novel<sup>3</sup>. The function of this unique domain is not understood. The N-terminal domain was initially thought to contain a catalytic site due to the presence of a zinc ion bound to this domain. Beta-carbonic anhydrases commonly complete zinc mediated catalysis<sup>3</sup>. In these enzymes, zinc is ligated to two cysteines and a histidine. The identity of the fourth ligand varies amongst the  $\beta$ -carbonic anhydrases; in CsoSCA the fourth ligand is a water molecule. An aspartate residue (Asp-175) competes with water for binding with zinc and makes catalysis more favorable by assuming a catalytically competent binding geometry for the incoming bicarbonate. However, the zinc found in the N-terminal domain of CsoSCA was determined to be the result of mutation in the cloned recombinant CsoSCA used and was deemed not biologically relevant<sup>3</sup>. The three residues (two cysteines and a histidine) that coordinate the zinc are not evolutionarily conserved in this domain so the initial notion that this domain may participate in catalytic function was dismissed. By removing the

first fifty amino acids of the N-terminal domain, this study will assess the necessity of this domain for incorporation of CsoSCA into the carboxysome and for the catalytic function of CsoSCA. Further insight into the structure/function relationship of CsoSCA can be gained, giving a better understanding of this crucial enzyme in carboxysome self-assembly and function.

### *Chapter III: Materials and Methods*

#### **Materials**

##### *Media*

##### **Luria-Bertani Broth (LB Broth) (pH 7.5)**

10 g/L NaCl  
10 g/L Bacto tryptone  
5 g/L Bacto yeast extract

##### **Luria-Bertani Agar (LBA) (pH 7.5)**

15 g/L Agar  
10 g/L Bacto tryptone  
10 g/L NaCl  
5 g/L Bacto yeast extract

##### **S.O.C. Medium (pH 7.0)**

20 g/L Bacto tryptone  
5 g/L Bacto yeast extract  
20 mM Glucose  
10 mM NaCl  
10 mM MgCl<sub>2</sub>  
10 mM MgSO<sub>4</sub>  
2.5 mM KCl

##### **Growth Medium for *H. neapolitanus* Liquid Cultures (pH 6.8)**

4 g/L KH<sub>2</sub>PO<sub>4</sub>  
4 g/L K<sub>2</sub>HPO<sub>4</sub>  
0.4 g/L NH<sub>4</sub>Cl  
0.4 g/L MgSO<sub>4</sub>  
10 g/L Na<sub>2</sub>S<sub>2</sub>O<sub>3</sub>•5H<sub>2</sub>O  
10 ml/L Trace element solution

##### **Growth Medium for *H. neapolitanus* Agar Plates (pH 6.8)**

0.2 g/L KH<sub>2</sub>PO<sub>4</sub>  
0.8 g/L K<sub>2</sub>HPO<sub>4</sub>  
0.01 g/L CaCl<sub>2</sub>  
1 g/L NH<sub>4</sub>Cl  
0.24 g/L MgSO<sub>4</sub>  
10 g/L Na<sub>2</sub>S<sub>2</sub>O<sub>3</sub>•5H<sub>2</sub>O  
15 g/L Agar  
1 ml/L Trace element solution  
4 ml/L 1% (m/v) Phenol red solution

**Trace Element Solution (pH 6.8)**

50 g/L EDTA  
5.44 g/L CaCl<sub>2</sub>  
1.61 g/L CoCl<sub>2</sub>  
1.57 g/L CuSO<sub>4</sub>•5H<sub>2</sub>O  
4.99 g/L FeSO<sub>4</sub>•7H<sub>2</sub>O  
5.06 g/L MnCl<sub>2</sub>•4H<sub>2</sub>O  
1.10 g/L (NH<sub>4</sub>)<sub>6</sub>Mo<sub>7</sub>O<sub>24</sub>•4H<sub>2</sub>O  
2.20 g/L ZnSO<sub>4</sub>•7H<sub>2</sub>O

*Dyes***Ethidium Bromide 1% (10 mg/mL)**

Fisher BioReagents

**6X Gel Loading Dye Blue**

New England Biolabs

*Buffers***TBE Buffer (pH 8.0)**

108 g/L Tris-base  
55 g/L Boric acid  
40 mL 0.5 M EDTA

**10X TE Buffer**

100 mM Tris-HCl (desired pH)  
10 mM EDTA (pH 8.0)

*Antibiotic Solutions*

**100 mg/mL Ampicillin in H<sub>2</sub>O (final working concentration: 100 µg/mL)**

**50 mg/mL Kanamycin in H<sub>2</sub>O (final working concentration: 50 µg/mL)**

*Plasmids and E. coli Strains*

*csoS3* pPROEX HTb-Top 10 – template DNA

TOPO kan cassette – template DNA

pTncsoS2::*csoS3* in pT7-6 vector – DNA sharing homology with the designed construct and used as acceptor for homologous recombination with the construct

pCR Blunt II-TOPO – cloning vector for insert of the designed DNA construct

One Shot Top 10 chemically competent *E. coli* – transformation with the DNA construct

pUC18 plasmid DNA – ligation with the DNA construct  
*E. coli* DY330 – homologous recombination host (overexpressed lambda recombinase)

## Methods

Polymerase chain reactions (PCRs) were completed to separately amplify a truncated *csoS3* gene and a kanamycin resistance cassette. A kan cassette was used as a selective marker; the bacteria in which the endogenous *csoS3* gene has been replaced with the construct can be identified through this marker. A technique known as overlap extension PCR was used to combine these two amplified fragments. Primers were specifically designed and are discussed in the Results section.

The DNA fragments, which consisted of the truncated *csoS3* gene and the kan cassette, were denatured and allowed to anneal through the short regions of complementary sequence engineered into the primers. PCR was repeated to allow the overlap region to be extended and to amplify the final DNA fragment. The fragment was cloned and the resulting plasmid was used for homologous recombination into a cloned piece of *H. neapolitanus* DNA. *E. coli* strain DY330 overexpresses bacteriophage lambda recombinase, which increases the rate of genetic recombination<sup>8</sup>. The resulting recombined plasmid DNA was used for *in vivo* recombination with the *H. neapolitanus* DNA<sup>9</sup>. Kanamycin resistant *H. neapolitanus* were selected. When *in vivo* gene replacement by homologous recombination was successful, growth curves for this mutant were measured and compared against those of wild type bacteria and a deletion mutant to determine if the truncation in the *csoS3* gene affected cell viability.

## ***Overlap Extension Polymerase Chain Reaction***

### *Preparing Overnight Cultures*

To prepare overnight cultures, 5 mL of LB medium and 5  $\mu$ L of ampicillin or other appropriate antibiotic stock solution were added to a polystyrene tube. A loop was sterilized and touched to the culture of cells needed (either from a glycerol stock or an LBA plate). The loop was placed into the tube containing LB and antibiotic and mixed gently. Tubes were incubated overnight at 37 °C, shaking (220 rpm). Turbidity indicates cell growth.

Overnight cultures were prepared for *E. coli* containing pTncsoS2::*csoS3* in pT7-6 vector as well as *csoS3* pPROEX HTb.

### *Isolation of Plasmids*

A QIAprep Spin Miniprep Kit (QIAGEN) was used to isolate plasmids. Concentrations (ng/ $\mu$ L) of the isolated plasmids were measured using a Nanodrop ND-1000 Spectrophotometer. The absorbance was measured and Beer's Law could be used to determine concentration.

### *PCR 1 and 2*

**Table 1** shows the reaction mixtures of PCR 1 and PCR 2, the reactions used to separately amplify the two fragments to be used in the overlap extension. These mixtures were prepared on ice. **Table 2** and **Table 3** show the PCR parameters for PCR 1 and PCR 2, respectively. PCR reactions were completed in a BioRad thermal cycler, which performed PCR based on the programmed parameters.

**Table 1. PCR 1 and 2 Reaction Mixtures**

	<b>PCR 1</b>	<b>PCR 2</b>
GoTaq Green Master Mix, 2X	10 $\mu$ L	10 $\mu$ L
Forward Primer (10 $\mu$ M)	1 $\mu$ L	1 $\mu$ L
Reverse Primer (10 $\mu$ M)	1 $\mu$ L	1 $\mu$ L
Template <i>csoS3</i> pPROEX HTb (191.2 ng/ $\mu$ L) or Topo kan cassette (114.1 ng/ $\mu$ L)	<i>csoS3</i> pPROEX HTb 0.5 $\mu$ L	Topo kan cassette 1 $\mu$ L
H <sub>2</sub> O	7.5 $\mu$ L	7 $\mu$ L
<b>Total Volume</b>	20 $\mu$ L	20 $\mu$ L

**Table 2. PCR 1 Parameters**

<b>Temperature (<math>^{\circ}</math>C)</b>	<b>Time</b>	<b>Cycles</b>
98	30 sec	1
98	10 sec	
62	30 sec	30
72	30 sec	
72	5 min	1
12	$\infty$	

**Table 3. PCR 2 Parameters**

Temperature (°C)	Time	Cycles
98	30 sec	1
98	10 sec	
56	30 sec	5
72	30 sec	
98	10 sec	
70	30 sec	25
72	30 sec	
72	5 min	1
12	∞	

*Gel Electrophoresis*

Following the PCR 1 and 2 reactions, a 0.7% agarose gel was prepared in 1X TBE buffer with ethidium bromide to visualize the DNA that had been amplified. The gel was loaded with a 1 kb ladder and the PCR products (2  $\mu$ L of each). A 100 V electric field was applied through the gel, causing the DNA to migrate towards the positively charged electrode. Once the DNA had migrated about halfway down the gel, electrophoresis was stopped. The gel was removed and imaged under UV light.

*PCR 3*

The overlap extension PCR was completed at an annealing temperature gradient (**Table 8**). Five reactions were planned, and reaction mixtures were prepared as shown in

**Table 4.** For tubes 4 and 5, 0.5  $\mu\text{M}$  of forward primer and 0.5  $\mu\text{M}$  of reverse primer were added after the first 4 amplification cycles. The total volume was 20  $\mu\text{L}$ . **Table 5** shows the parameters of PCR 3.

**Table 4. PCR 3 Reaction Mixtures**

	<b>Tubes 1, 2, and 3</b>	<b>Tubes 4 and 5</b>
GoTaq Green Master Mix, 2X	10 $\mu\text{L}$	10 $\mu\text{L}$
Forward Primer (10 $\mu\text{M}$ )	1 $\mu\text{L}$	0 $\mu\text{L}$
Reverse Primer (10 $\mu\text{M}$ )	1 $\mu\text{L}$	0 $\mu\text{L}$
Template	0.5 $\mu\text{L}$ from PCR 1 0.5 $\mu\text{L}$ from PCR 2	0.5 $\mu\text{L}$ from PCR 1 0.5 $\mu\text{L}$ from PCR 2
H <sub>2</sub> O	7 $\mu\text{L}$	7 $\mu\text{L}$
<b>Total Volume</b>	20 $\mu\text{L}$	18 $\mu\text{L}$

Template concentrations were not determined. PCR purification was not completed for PCR 1 and 2 products, and their concentrations were not quantified.

**Table 5. PCR 3 Parameters**

<b>Temperature (<math>^{\circ}\text{C}</math>)</b>	<b>Time</b>	<b>Cycles</b>
98	30 sec	1
98	10 sec	
56-66*	30 sec	4
72	40 sec	
98	10 sec	

56-66	30 sec	26
72	40 sec	
72	5 min	1
12	$\infty$	
<b>*See Table 8 for the annealing temperature gradient.</b>		

After PCR was complete, the PCR products were visualized using gel electrophoresis on a 0.7% agarose gel.

#### *Gel Excision and Purification*

To recover the DNA, gel excision and purification processes were used. A fresh preparative gel electrophoresis was completed. Bands were visualized using a UV light, and the desired bands were excised using a blade. The QIAEX II Gel Extraction Kit from QIAGEN was used to isolate the DNA. The concentration of the DNA extracted was measured using the Nanodrop ND-1000 Spectrophotometer.

#### ***Cloning and Recombination in E. coli DY330***

##### *Cloning and Transformation of Top 10 cells*

The fragment generated by overlap extension PCR underwent a TOPO cloning reaction. TOPO cloning is a technique that is used to efficiently clone blunt-ended PCR products into the pCR Blunt II-TOPO vector. One Shot chemically competent Top 10 cells were then transformed with the TOPO plasmid. To set up the TOPO cloning reaction, 4  $\mu$ L of fresh PCR product, 1  $\mu$ L of salt solution, and 1  $\mu$ L of pCR Blunt II-

TOPO vector were added together in that order. The reaction was mixed gently and incubated for 5 minutes at room temperature. This reaction was then placed on ice. Once ready to transform chemically competent cells, the vial was centrifuged and then placed back on the ice. A vial of chemically competent One Shot Top 10 cells was thawing on the ice. To the vial, 5  $\mu$ L of the cloning reaction were added. The vial was mixed by tapping it gently. The vial was incubated on ice for 30 minutes. The vial was then removed from the ice and incubated for 30 seconds in a 42 °C water bath. The vial was removed from the bath and placed back on ice. Next, 250  $\mu$ L of S.O.C. medium (pre-warmed to 23 °C) were added to the vial. The vial was then placed in a shaking incubator, taped to lie on its side. The vial remained shaking at 225 rpm for 1 hour at 37 °C. Once removed, 40  $\mu$ L of the mixture were spread using aseptic measures on a Luria-Bertani Agar (LBA) plate containing kanamycin in the medium. The plate was incubated overnight at 37 °C.

#### *PCR Screening of Transformants*

Eight colonies (transformants) from the plate were selected for PCR screening. Eight microcentrifuge tubes were filled with 50  $\mu$ L of TE Buffer, and an LBA plate containing kanamycin was divided into eight sections. Using a sterilized loop, a single colony was selected. The loop was placed into the TE Buffer and was gently moved around. The loop was then used to streak the corresponding section of the LBA plate. The loop was re-sterilized in ethanol and flamed. This process was completed for each selected colony. The plate was placed in the 37 °C stationary incubator. The microcentrifuge tubes were incubated for 1 minute at 100 °C. A PCR master mix was

prepared by combining 90  $\mu\text{L}$  GoTaq, 9  $\mu\text{L}$  M13F(-20) primer, 9  $\mu\text{L}$  M13 reverse primer, and 63  $\mu\text{L}$  H<sub>2</sub>O. Nineteen  $\mu\text{L}$  aliquots of the mix were pipetted into 8 PCR tubes. The contents of the eight microcentrifuge tubes containing TE Buffer and selected colonies were used as template DNA for the PCR screening. One  $\mu\text{L}$  of template was pipetted into the corresponding PCR tube. PCR was completed using the parameters outlined in **Table 6**.

**Table 6. PCR Screening Parameters**

Temperature ( $^{\circ}\text{C}$ )	Time	Cycles
95	2 min	1
95	30 sec	
56	30 sec	30
72	2 min	
72	5 min	1
12	$\infty$	

Following PCR, PCR products were loaded into a 0.7% agarose gel, and gel electrophoresis was completed. The gel was visualized under ultraviolet light.

#### *Sequencing of Ppositive Transformants*

Positive transformants identified through PCR screening were sent for sequencing to Eurofins Genomics with M13F(-20) primer, M13 reverse primer, and S3r5545 primer.

#### *Enzyme Restriction Reaction*

EcoR1 was identified as a restriction enzyme that would cut the fragment out of the plasmid vector without cutting the fragment itself. **Table 7** shows the reaction

mixture used for enzyme restriction. The restriction reactions were loaded into a gel, and gel electrophoresis procedures were completed. The desired fragments were excised and gel purified. Concentrations were measured on the Nanodrop ND-1000 Spectrophotometer.

**Table 7.** Enzyme Restriction Reaction

<b>Reagents</b>	<b>Amount</b>
Buffer	3.75 $\mu$ L
Restriction Enzyme	3 $\mu$ L
Plasmid	3 $\mu$ g
Water	Up to 30 $\mu$ L
<b>Total Volume</b>	30 $\mu$ L

*Electroporation of E. coli DY330 Cells*

Overnight cultures of DY330 were incubated at 30 °C. A 50 mL subculture was inoculated with 1:50 of overnight culture and incubated at 220 rpm until the OD<sub>600</sub> reached 0.477. Next, 25 mL of this culture were transferred to a 250 mL flask and incubated in a 42 °C water bath with shaking for 15 minutes. The flask was transferred to an ice-water slurry to shake and cool for 15 minutes. The cells were then harvested by centrifuging at 4000 rpm using the JA-25.50 rotor for 10 minutes at 4 °C. The supernatant was discarded, and the cells were resuspended in 1 mL of ice-cold H<sub>2</sub>O and transferred to a 1.5 mL tube. The tube was centrifuged at 14,000 rpm for 20 seconds at 4 °C. The supernatant was discarded, and the pellet again was resuspended in 1 mL of ice-cold

H<sub>2</sub>O. The centrifugation was repeated an additional two times, and the final cell pellet was resuspended in 200  $\mu$ L of ice-cold water. The cells were kept on ice.

For the electroporation, 1  $\mu$ g of the linear donor DNA (the construct) and 1  $\mu$ g of the plasmid acceptor DNA (pTncsoS2::*csoS3*) were added to a 0.1 cm gap, pre-cooled electroporation cuvette. *E. coli* DY330 (100  $\mu$ L) was added to the cuvette, and the cuvette was tapped to disperse bubbles. The cells were electroporated at 2.0 kV, 25  $\mu$ F, and 200  $\Omega$  (peak voltage: 1902 V). The cuvette was removed, and 1 mL of LB medium was immediately added. The cell suspension was transferred to a round-bottomed Falcon tube and incubated on ice for 5 minutes. The tube was transferred to a 30 °C shaker for 1.5 hours. A 200  $\mu$ L aliquot was spread on an LBA plate with kanamycin, and the remaining suspension was spread on an LBA plate with ampicillin as control. Transformants were selected for PCR screening, and the parameters in **Table 6** were used. Positive transformants were sent to Eurofins Genomics for sequencing using the same primers discussed previously.

### ***Gene Replacement in H. neapolitanus***

An enzyme digest was completed on the purified plasmid DNA of the positive recombinant (designed construct recombined in pTncsoS2::*csoS3*) identified by screening and sequencing. HindIII and PstI were used to cut the vector around the construct. The pUC 18 vector was also treated with the same enzymes to linearize the DNA. Restriction reactions were loaded onto a gel, and the desired bands were excised and purified. Next, a ligation was completed by adding 25 ng of vector DNA, 75 ng of insert DNA, 1  $\mu$ L of 10X ligase buffer, and 1  $\mu$ L ligase. Top 10 cells were transformed with the ligation. The transformation mixtures were plated, and colonies were selected for screening. As

completed with *E. coli* DY330, an electroporation of *H. neapolitanus* was completed. *H. neapolitanus* mutants were screened and sequenced.

### ***Growth Curves of H. neapolitanus***

Growth curves were started by first adding a 5 mL culture of each cell type (wildtype, deletion mutant, and truncated mutant) with 5 µL kanamycin (except wildtype) and placing them in a 30 °C shaking incubator. The cultures were incubated until growth was indicated by an increase in OD<sub>600</sub> value (wildtype: 0.0705; deletion mutant: 0.0836; truncated mutant: 0.0836). *H. neapolitanus* liquid growth medium (50 mL) was added to 12 flasks. Into 4 flasks, 200 µL of wildtype culture was added. To 4 flasks, 168.7 µL of deletion mutant was added. To the final four flasks, 173.6 µL of truncated mutant was added. Duplicate cultures of each cell type were added to the 30 °C incubator containing air and the 30 °C incubator containing air enriched with 5% CO<sub>2</sub>. The OD<sub>600</sub> was measured at various time points by centrifuging 1 mL of culture from each flask for 5 seconds and using the top 500 µL for the OD<sub>600</sub> reading.

## ***Chapter IV: Results***

The goal of this project was to produce a construct for gene replacement in *Halothiobacillus neapolitanus*. The construct was designed so that amino acids M1-R50, the first 50 amino acids of the N-terminal domain of the *csoS3* gene, were removed. The desired final product will have a 41 nucleotide handle from the upstream *csoS2* gene for homologous recombination, a kanamycin resistance cassette, a Shine-Dalgarno sequence upstream of the *csoS3* gene, and the truncated *csoS3* gene, as demonstrated in **Figure 6**. A short region of homology is required for recombination of linear DNA in *Escherichia*

*coli* DY330. For this reason, a forty-one nucleotide handle from the 3'-end of *csoS2* was included in the design. The kanamycin resistance cassette was inserted for selection of mutants exhibiting a successful recombination. The Shine-Dalgarno sequence is necessary for recruitment of the ribosome to mRNA for initiation of translation. This sequence also contains the ATG start codon. The N-terminal sequence was truncated by deleting 150 nucleotides in order to produce a deletion construct without M1-R50. A portion of the middle domain of *csoS3* was included for homology to promote recombination.

**Desired Final Product:**



S2- 41 nucleotide handle

Kan<sup>R</sup>- kanamycin resistance cassette

SD- Shine Dalgarno sequence before the *csoS3* gene

NTD-S3 – Starting at H51 of NTD-S3 of *csoS3*

MD-S3 – Middle domain of *csoS3*

**Figure 6. Construct Design.** The desired final product was designed specifically for deletion of the first fifty amino acids of the N-terminal domain of *csoS3* and for the inclusion of the kanamycin resistance cassette.

The following flowchart (**Figure 7**) visually demonstrates how this goal was accomplished.

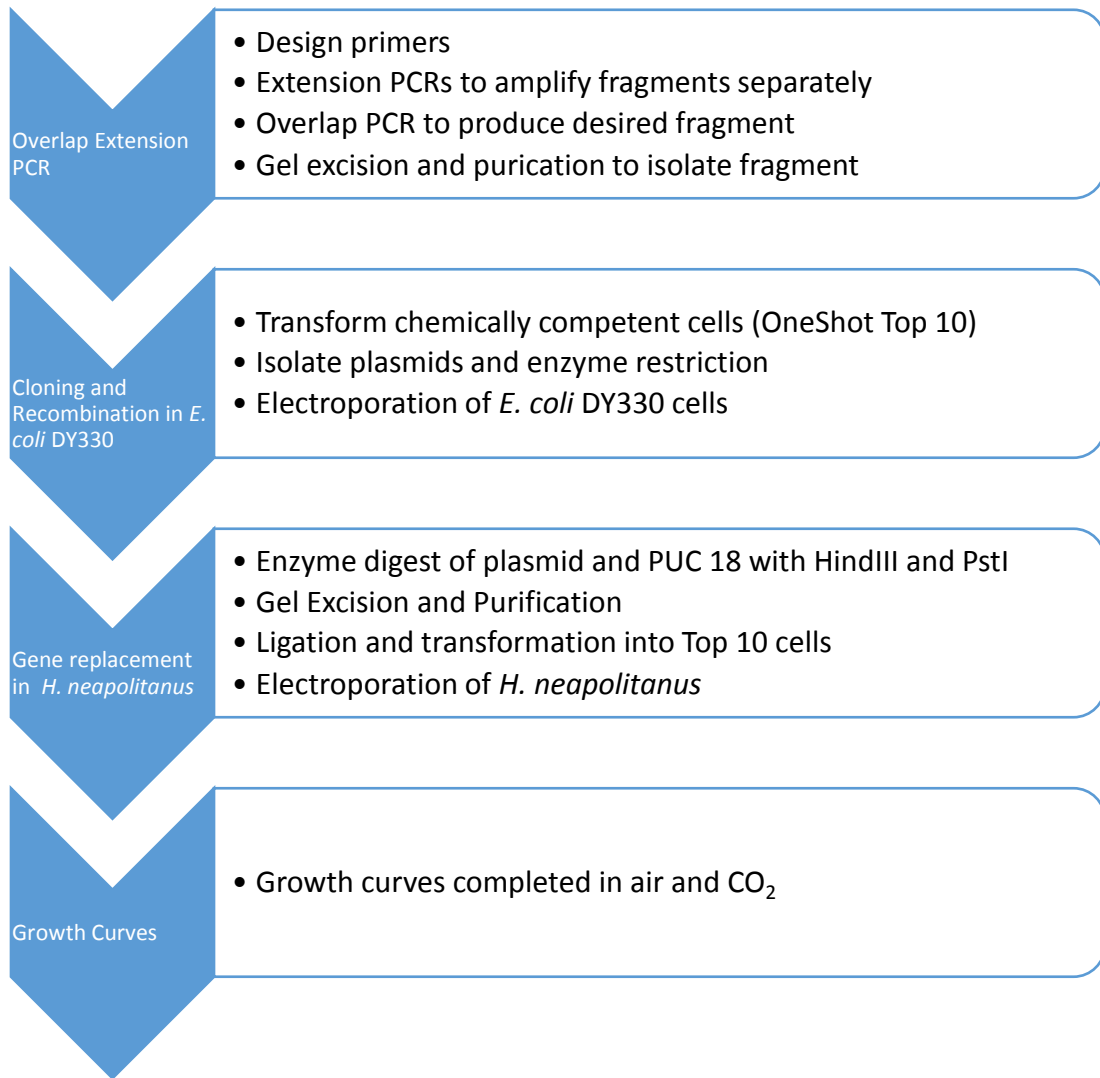


**Figure 7. Flow Chart.** The flow chart displays the experimental design used to achieve the project goal.

### ***Overlap Extension Polymerase Chain Reaction***

To make this construct, an overlap extension polymerase chain reaction with specifically designed primers was used to combine the truncated *csoS3* gene with the kanamycin cassette. Primers were designed using OligoAnalyzer 3.1, a primer design tool provided by Integrated DNA Technologies (<https://www.idtdna.com/site>). Three

polymerase chain reactions were completed for the overlap extension. PCR 1 and PCR 2 were performed to produce the two fragments needed for the overlap extension. PCR 3 is the overlap extension PCR. **Figures 8, 9, and 10** show the primer designs.

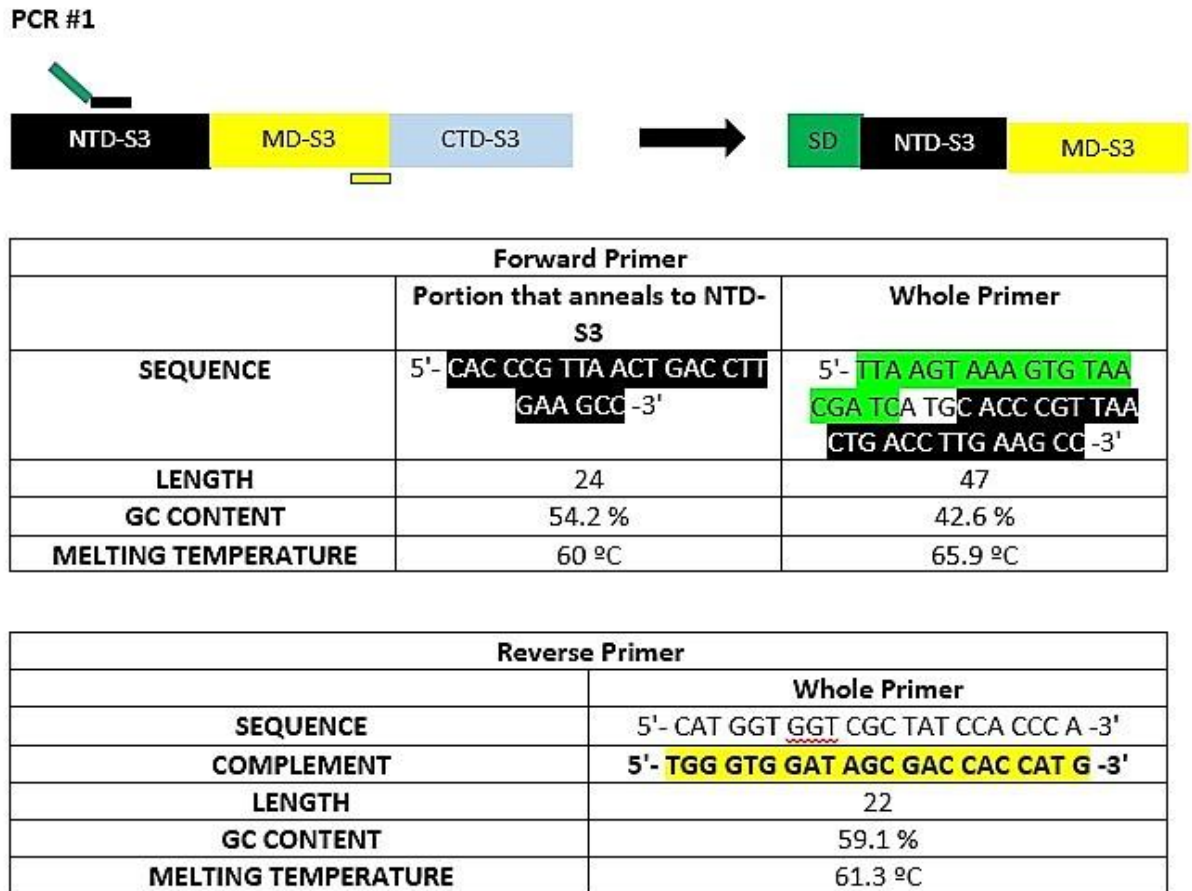
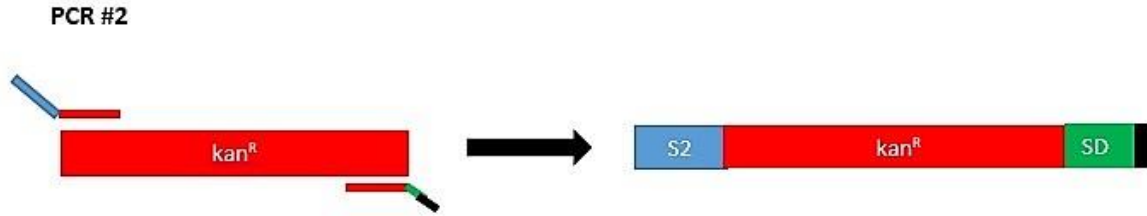


**Figure 8. Primer Design for PCR 1.** The forward primer was designed to anneal to the 151<sup>st</sup> base pair in the *csoS3* N-terminal domain coding sequence. The forward primer also includes a Shine-Dalgarno sequence so the ribosome can be recruited to the mRNA and translate efficiently. The reverse primer was designed to anneal to a sequence towards the 3'-end of the middle domain of *csoS3*.

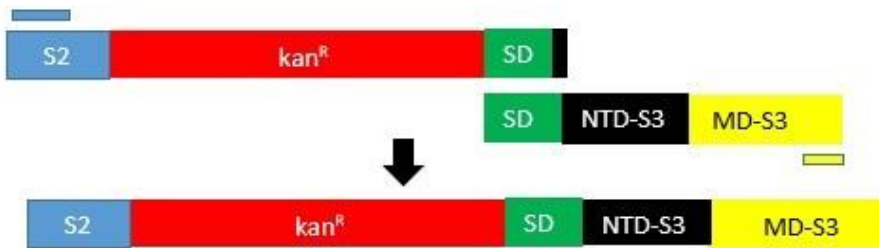


Forward Primer		
	Portion that anneals to kan	Whole Primer
SEQUENCE	5'- CCG GAA TTG CCA GCT G - 3'	5'- AAG GTA GTC TGA TCA CTT ACT CCG GCG GCG CGC GCG GTT GAC CCG AAT TGC CAG CTG -3'
LENGTH	16	57
GC CONTENT	62.5 %	61.4 %
MELTING TEMPERATURE	54.1 °C	74.7 °C

Reverse Primer		
	Portion that anneals to kan	Whole Primer
SEQUENCE	5'- CTA TCG CCT TCT TGA CGA GTT CTT CTG A -3'	5'- CTA TCG CCT TCT TGA CGA GTT CTT CTG ATT AAG TAA AGT GTA ACG ATC ATG CAC CCG T -3'
COMPLEMENT	5'- TCA GAA GAA CTC GTC AAG AAG GCG ATA G -3'	5'- ACG GGT GCA TGA TCG TTA CAC TTT ACT TAA TCA GAA GAA CTC GTC AAG AAG GCG ATA G -3'
LENGTH	28	58
GC CONTENT	46.4 %	43.1 %
MELTING TEMPERATURE	59.5 °C	67.5 °C

**Figure 9. Primer Design for PCR 2.** The forward primer was designed to anneal to the 5'-end of the kanamycin resistance cassette sequence, and the reverse primer was designed to anneal to the 3'-end of the kanamycin resistance cassette sequence. The forward primer also includes a *csoS2* tail, and the reverse primer includes a Shine-Dalgarno and *csoS3* N-terminal sequence tail.

**PCR #3**



Forward Primer	
	<b>Whole Primer</b>
<b>SEQUENCE</b>	5'- ACC CAA GGT AGT CTG ATC ACT TAC TCC GG -3'
<b>LENGTH</b>	29
<b>GC CONTENT</b>	51.7 %
<b>MELTING TEMPERATURE</b>	62.2 °C

**\*\*We will use the reverse primer used in PCR #1. \*\***

Reverse Primer	
	<b>Whole Primer</b>
<b>SEQUENCE</b>	5'- CAT GGT GGT CGC TAT CCA CCC A -3'
<b>COMPLEMENT</b>	5'- TGG GTG GAT AGC GAC CAC CAT G -3'
<b>LENGTH</b>	22
<b>GC CONTENT</b>	59.1 %
<b>MELTING TEMPERATURE</b>	61.3 °C

**Figure 10. Primer Design for PCR 3.** The forward primer was designed to anneal to *csoS2*, making ta handle for homology. The reverse primer is the same reverse primer used in PCR 1.

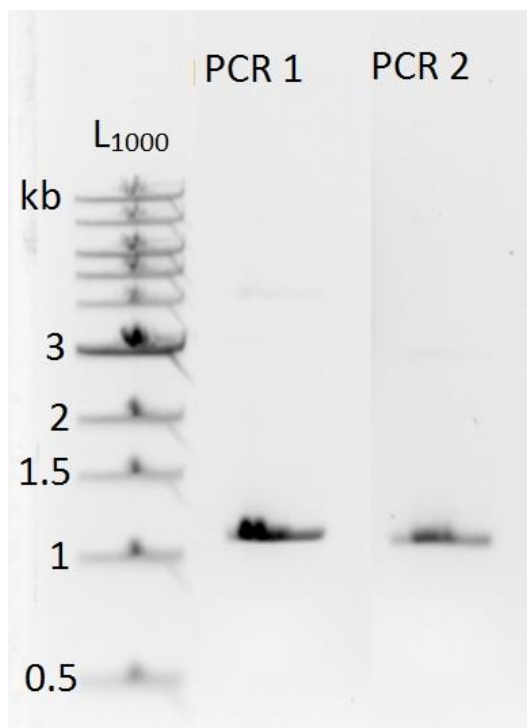


**Figure 11. Analytical Gel Electrophoresis of PCR Products.** The expected fragment size for PCR 1 is 1050 bp while the expected fragment size for PCR 2 is 933 bp. L<sub>1000</sub> is a 1000 bp DNA size ladder. The image is a composite. Lanes not relevant to the experiment were excised. Because the middle lanes were cropped, retardation of the migration in lanes on the border of the gel make the band in the PCR 2 lane to appear larger than it is.

The third polymerase chain reaction was the overlap extension and was completed using a temperature gradient (**Table 8**) to optimize the specificity of primer annealing. Reactions in tubes 3 and 4 showed bands (of approximately 2 kb) with the greatest intensity indicating that these reactions yielded the most PCR product of the expected size of 2028 bp (**Figure 12**). The optimized temperature of primer annealing then was determined to be 59.7 °C. The reaction was also favorable when the second annealing temperature was increased to 66 °C.

**Table 8. Overlap Extension PCR Temperature Gradient (°C)**

PCR Annealing Temperature Gradient					
Tube	1	2	3	4*	5*
T <sub>A1</sub>	56 °C	57.9 °C	59.7 °C	59.7 °C	59.7 °C
T <sub>A2</sub>	56 °C	57.9 °C	59.7 °C	59.7 °C	66 °C
*Primers were added after the first 4 cycles of PCR					

**Table 8. PCR Annealing Temperature Gradient.** T<sub>A1</sub> is the first annealing temperature, and T<sub>A2</sub> is the second annealing temperature.

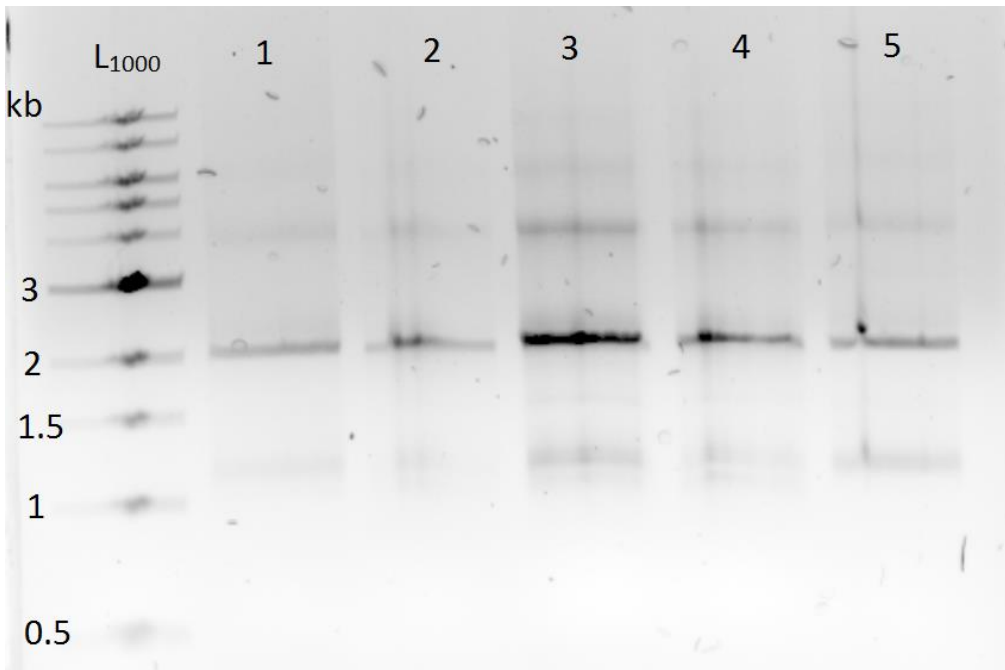


**Figure 12. Analytical Gel Electrophoresis of the Overlap Extension PCR.** The expected fragment size for the overlap extension was 2028 bp. A temperature gradient was used to complete this PCR. Refer to Table 8 for annealing temperatures. L<sub>1000</sub> is a 1000 bp DNA size ladder.

Because reactions 3 and 4 yielded the most PCR product of approximately 2 kb, the remaining PCR volumes (18  $\mu$ L of each) were loaded onto a gel for preparative

electrophoresis and band excision (**Figure 13**). The bands were excised to isolate the desired DNA fragment produced by the overlap extension.

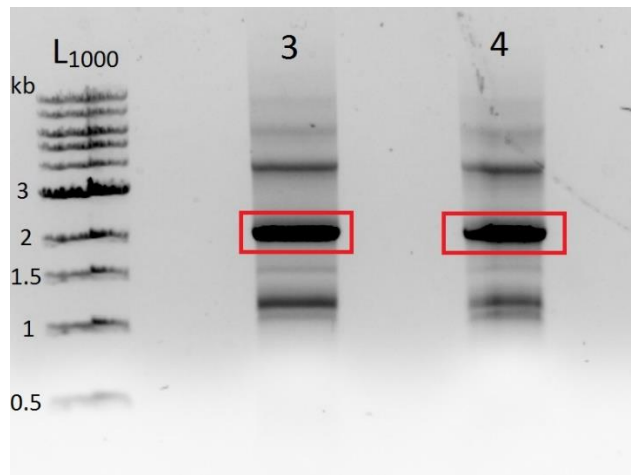


**Figure 13. Preparative Gel Electrophoresis of Reactions 3 and 4 of the Overlap Extension PCR.** For each reaction, 18  $\mu\text{L}$  (remaining volume) and 3  $\mu\text{L}$  of loading dye were loaded onto a freshly prepared 0.7% agarose gel. The fragments of approximately 2 kb (indicated by the boxes) were excised from the gel. L<sub>1000</sub> is a 1000 bp DNA size ladder.

After excision and purification, concentrations of the extracted DNA were determined to be 15.0 ng/ $\mu\text{L}$  for reaction 3 and 18.4 ng/ $\mu\text{L}$  for reaction 4.

### ***Cloning and Recombination in E. coli DY330***

Electrocompetent *E. coli* DY330 were used for initial recombination. This bacterial strain was used over direct recombination in *H. neapolitanus* because the bacteriophage-encoded  $\lambda$  recombinase of *E. coli* can recombine sequences with homologies from 30 to 50 bases<sup>8</sup>, whereas the recombination machinery of *H. neapolitanus* requires longer stretches of homology. **Figure 9** shows the homologous recombination event that was expected to occur.

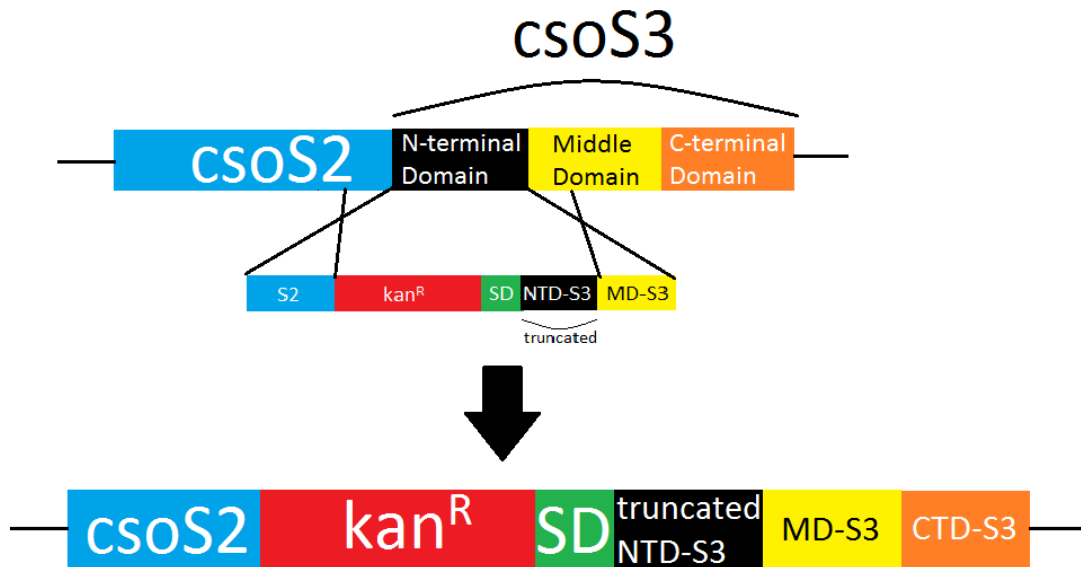


**Figure 14. Homologous Recombination.** The image presents the expected recombination event accomplished through electroporation of *E. coli* DY330. The construct produced by overlap extension PCR was recombined with the pTncsoS2::csoS3 plasmid (vector = pT7-6) in *E. coli* DY330.

Before the electroporation of *E. coli* DY330 could be completed, the linear fragment DNA had to be inserted into a plasmid cloning vector (TOPO) that included an origin of replication so that the host bacteria could copy the circular DNA. Once transformed with the chemically competent cells, electroporation was used to send a pulse of electricity through the cell, opening pores in the membrane. The overlap extension fragment and the pTncsoS2::csoS3 plasmid were pulled through these pores, and recombination occurred.

Once the fragment was incorporated into the TOPO cloning vector, and the TOPO plasmids were used to transform chemically competent Top 10 cells, A PCR screening was completed as shown in **Figure 15**.

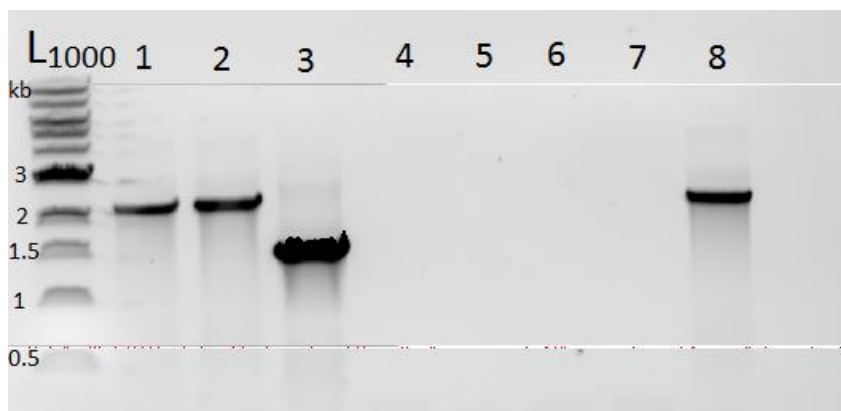


**Figure 15. PCR Screening of *E. coli* Top 10 Transformants.** The expected fragment size of transformants was 2272 base pairs. L<sub>1000</sub> is a 1000 bp DNA size ladder.

Colonies 1, 2, and 8 were identified as potentially positive clones based on similarities in size of the transformants compared with the expected size of 2272 bases. Overnight cultures were prepared for clones 2 and 8. Sequencing of the DNA isolated from these clones indicated that the expected fragment produced by overlap extension PCR was present and had the sequence that was anticipated. Once this was corroborated, electroporation of *E. coli* DY330 could be completed.

Enzyme restriction reactions with EcoR1 of the plasmid DNA isolated from the positive clones were completed in order to produce the linear DNA donor needed for electroporation. These reactions were loaded onto a gel, and desired fragments were excised and purified. After purification, the concentration of DNA of the EcoR1 digest of the plasmid DNA isolated from colony 8 (12.2 ng/μL) was higher than the concentration of DNA of the EcoR1 digestion of the plasmid DNA isolated from colony 2 (9.3 ng/μL), so the plasmid DNA from colony 8 was used as the linear donor. The acceptor DNA was pTnc<sub>so</sub>S2::*csoS3* in pT7-6 vector (63.4 ng/μL). This electroporation proved to be unsuccessful, having a small yield of negative recombinants.

To improve the results of the electroporation, a PCR was completed for amplification of linear fragment donor DNA. **Figure 16** shows the result of this PCR.

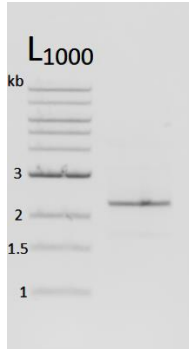


**Figure 16. Linear Donor Fragment after Amplification by PCR.** Because the first electroporation was unsuccessful, it was predicted that a low concentration of the linear donor fragment could be the cause of low colony yield. The linear donor fragment was amplified by using plasmid DNA isolated from colony 2 as the template. Upon isolation of the donor fragment, a concentration of 30.5 ng/ $\mu$ L was obtained. The initial electroporation used a linear donor fragment of 12.2 ng/ $\mu$ L.

Electroporation was completed with the new linear donor fragment (30.5 ng/ $\mu$ L) and pTncsoS2::*csoS3* in pT7-6 vector as the acceptor (63.4 ng/ $\mu$ L). In this second trial, 457.5 ng of the linear donor (15  $\mu$ L) were combined with 457.5 ng (7.22  $\mu$ L) of plasmid acceptor. After electroporation, numerous transformant colonies were present. Sixteen colonies were selected for PCR screening (labeled 4-35 as three colonies had been screened already in the first electroporation). **Figure 17** shows the PCR screening results for colonies 20-35.

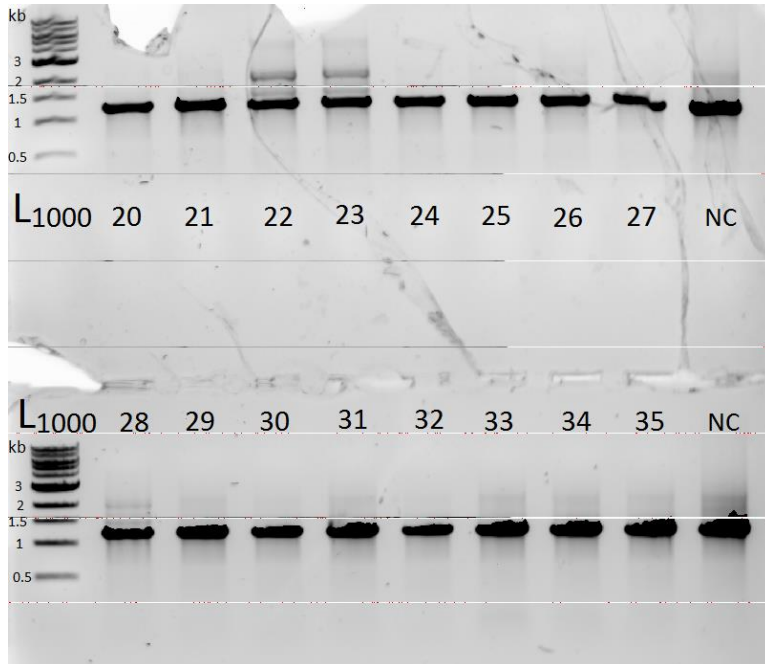


**Figure 17. PCR Screening of Transformant Colonies.** The expected fragment length was 2028 bp. If the kanamycin resistance cassette was recombined in the genome, the fragment length would be 2143 bp. A negative result, as indicated by the two final lanes labeled NC, would be 1242 bp. The negative control was the donor DNA fragment (shows no recombination). Colony 22 and 23 were identified as recombinants. L<sub>1000</sub> is a 1000 bp DNA size ladder.

The lanes labeled NC for negative control contained the donor DNA fragment. The negative control shows the band size that would result with no recombination. However if recombination occurred, a band was expected at 2143 bp. Colonies 22 and 23 were identified as a probable positive recombinants based on the presence of the fragment at approximately 2 kb. Two distinct bands are separated in these clones because they contain both recombined and original DNA.

### ***Gene Replacement in H. neapolitanus***

To begin preparation for the electroporation of *H. neapolitanus*, an overnight culture of clone 22 was prepared, and plasmid DNA was isolated. An enzyme digest

reaction was completed in order to isolate the recombinant fragment as well as pUC 18 vector for a ligation reaction. HindIII and PstI were identified as restriction enzymes that would cut plasmid 22 at the restriction sites directly upstream and directly downstream of the desired construct, excising it from the vector. These restriction enzymes would also linearize pUC18 for ligation. **Figure 18** shows the result of the enzyme digest.

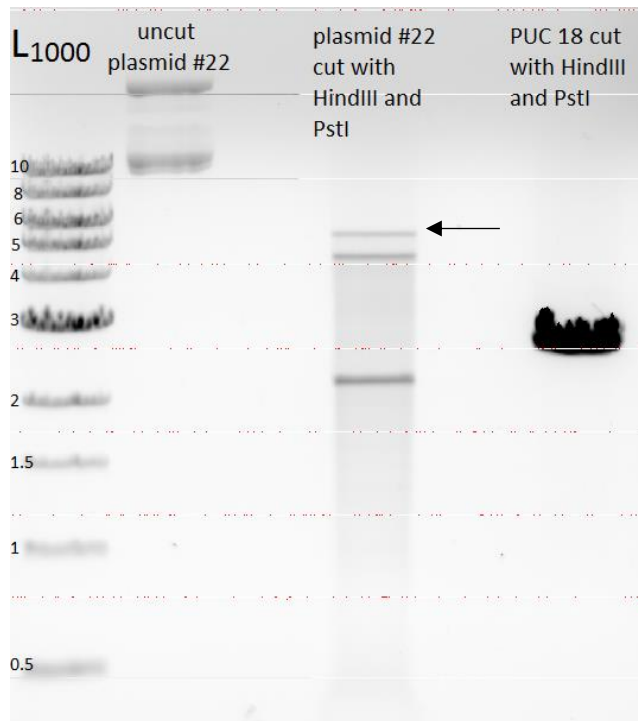


**Figure 18. Preparative Gel Electrophoresis of Enzyme Digest for Ligation Reaction.**

When cutting plasmid 22 with the restriction enzymes HindIII and PstI, the expected fragments were 2208 bp (size of the pT7-6 vector), 5040 bp (size of the recombinant fragment), and at 4157 bp (size of the pTncsoS2::csoS3 fragment indicating no recombination). The arrow indicates the recombinant fragment. The pUC 18 vector was linearized. A preparative 0.7% agarose gel was used for subsequent excision of the recombinant fragment and the linearized vector. L<sub>1000</sub> is a 1000 bp DNA size ladder.

The cut plasmid #22 band of approximately 5040 bp (indicated by the arrow) and the cut pUC 18 band were excised and gel purified. A ligation of the recombinant fragment and

the linearized pUC 18 vector was completed. The mixture was then used to transform chemically competent Top 10 cells (**Figure 19**).

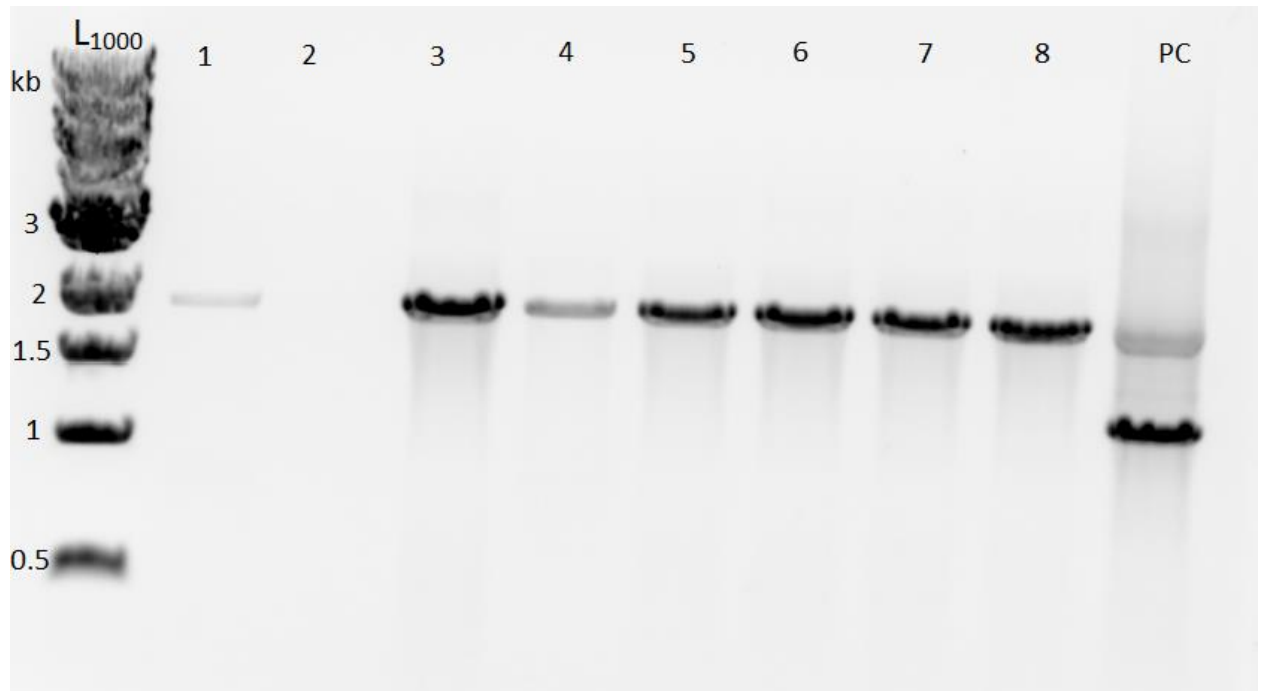


**Figure 19. Analytical Gel Electrophoresis of the *E. coli* Top 10 Transformants.** The expected band was 2028 bases. The positive control (PC) was DNA plasmid isolated from clone 22. Colonies 1 and 3-8 showed bands at around 2 kb that aligned with the top band of the positive control, indicating that they matched the size of the expected recombinant fragment. L<sub>1000</sub> is a 1000 bp DNA size ladder.

**Figure 19** shows that by excising the band identified as being potentially recombinant (**Figure 18**), the recombinant fragment was successfully isolated from the unrecombined DNA. An overnight culture of colony 8 was prepared, plasmids were isolated, and they were sent for sequencing. Sequencing further confirmed that colony 8 contained the desired designed construct.

To incorporate the confirmed recombinant construct into the *H. neapolitanus* genome, *H. neapolitanus* was electroporated. This generated several mutant colonies. Of

these, ten transformants were selected for PCR screening. **Figure 20** shows the results for colonies 4 and 5.

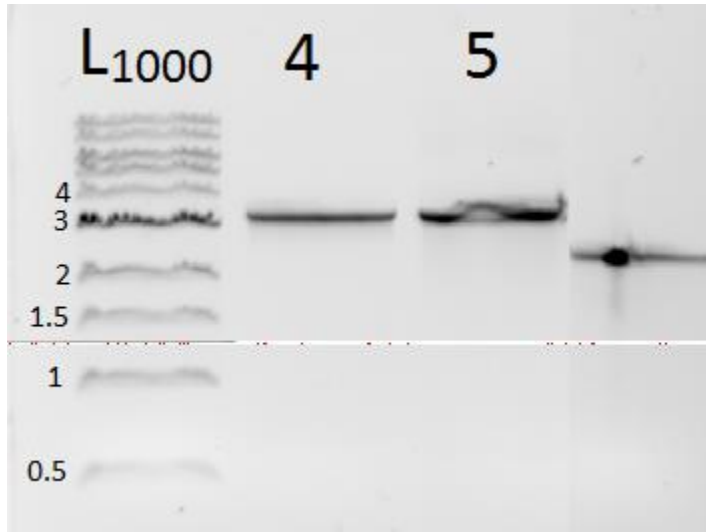


**Figure 20. Analytical Gel Electrophoresis of PCR Screening of *H. neapolitanus* Mutants 4 and 5.** The expected band size was 3238 bp. The negative control to the far right was *H. neapolitanus* genomic DNA. L<sub>1000</sub> is a 1000 bp DNA size ladder. The image is a composite.

If the designed construct had been incorporated into the genome, the PCR screening of DNA plasmids from the mutant colonies would have a band size of 3238 bp. Out of the ten colonies that were screened, five showed bands at approximately this size. DNA plasmids isolated from mutants 4 and 5 were sent for sequencing. Sequencing confirmed that the gene replacement with the desired construct in *H. neapolitanus* was successful.

### ***Growth Curves of H. neapolitanus***

Once it was verified that gene replacement had occurred, growth curves were started to compare the growth rates of *H. neapolitanus* wild type, a *csoS3* deletion mutant, and the truncated mutant constructed. For these growth curves, optical density

readings measured at a wavelength of 600 nm (OD<sub>600</sub>) were taken over time. This value is an estimation of bacterial concentration, so as the value increases, bacterial population growth has occurred. **Table 9** and **Figure 21** show growth curves with duplicates completed in air. **Table 10** and **Figure 22** show growth curves with duplicates completed in CO<sub>2</sub> enriched air. The duplicates were biological replicates; two clones of each type were used for the growth curves to ensure that outside variables were not affecting the growth rate.

**Table 9. Growth Curve Values for Wild Type, *csoS3* Deletion Mutant, and *csoS3* Truncated Mutant in Air**

	OD600					
	Air					
	WT1	S3 del 1	S3 trun 1	WT2	S3 del 2	S3 trun 2
Inc Time	1	2	3	4	5	6
0						
5	-0.0086	-0.0072	-0.0013	-0.0036	-0.0041	-0.008
11	0.0177	-0.0028	0.0064	0.0047	-0.0096	-0.0026
17	0.1008	0.0021	0.0211	0.0626	-0.0045	0.0237
28	0.0978	0.0172	0.0707	0.1094	0.0103	0.1054
32	0.1083	0.0248	0.076	0.1119	0.0177	0.1078
36	0.0982	0.0378	0.0771	0.1118	0.032	0.1087

Incubation (Inc) time was recorded as hours post inoculation.

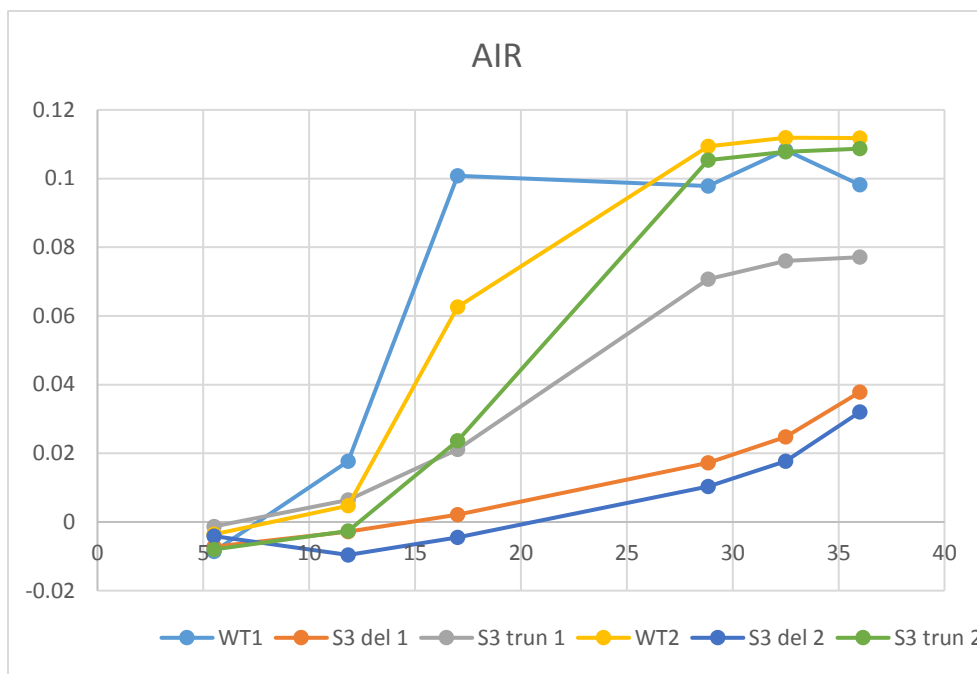


**Figure 21. Growth Curve Values for Wild Type, *csoS3* Deletion Mutant, and *csoS3* Truncated Mutant in Air.** Growth rates of wild type (WT1 and WT2), *csoS3* deletion mutant (S3 del 1 and S3 del 2), and *csoS3* truncated mutant (S3 trun 1 and S3 trun 2) in air are displayed graphically.

**Table 10. Growth Curve Values for Wild Type, *csoS3* Deletion Mutant, and *csoS3* Truncated Mutant (with Duplicates) in CO<sub>2</sub>**

	OD600					
	CO <sub>2</sub>					
	WT1	S3 del 1	S3 trun 1	WT2	S3 del 2	S3 trun 2
Inc Time	7	8	9	10	11	12
0						
5	-0.0068	0	-0.0101	-0.0134	-0.0085	-0.0035
12	0.0068	0.0157	0.019	0.0065	0.0081	0.0132
17	0.1637	0.0261	0.1085	0.1456	0.0183	0.084
29	0.1946	0.1808	0.1828	0.1952	0.1597	0.1768
32	0.1972	0.191	0.2096	0.196	0.1764	0.21
36	0.1964	0.2015	0.2228	0.198	0.1922	0.2168

Incubation (Inc) time was recorded as hours post inoculation.

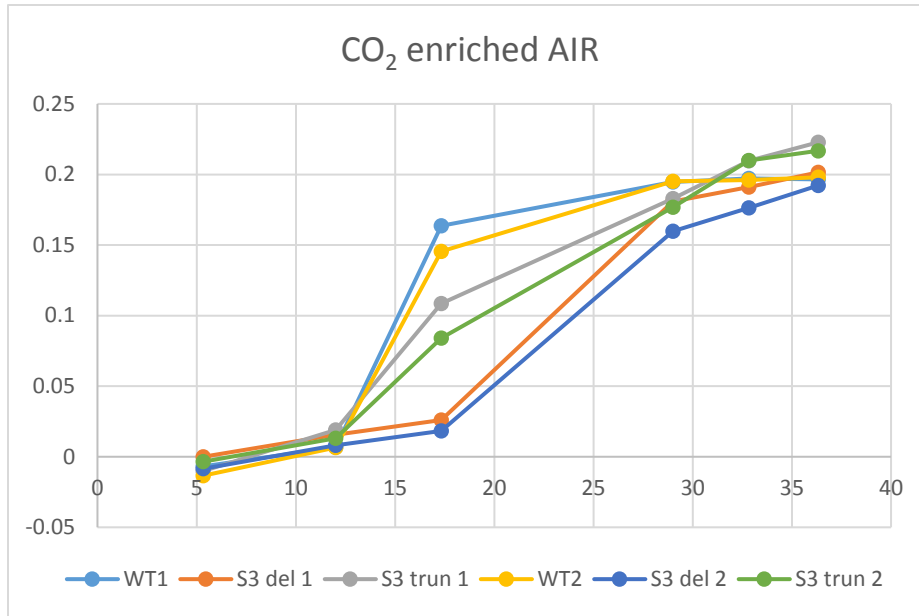


**Figure 22. Growth Curve Values for Wild Type, *csoS3* Deletion Mutant, and *csoS3* Truncated Mutant (with Duplicates) in CO<sub>2</sub>.** Growth rates of wild type (WT1 and WT2), *csoS3* deletion mutant (S3 del 1 and S3 del 2), and *csoS3* truncated mutant (S3 trun 1 and S3 trun 2) in CO<sub>2</sub> are displayed graphically.

*H. neapolitanus* wild type grows better than both mutants in both air and CO<sub>2</sub> enriched air. The *csoS3* truncated mutant grows better than the *csoS3* deletion mutant in both air and CO<sub>2</sub> enriched air but considerably better than the *csoS3* deletion mutant in air.

## *Chapter V: Discussion and Conclusion*

Carboxysomal carbonic anhydrase, CsoSCA, of *H. neapolitanus* was chosen as the focus of this study because of its novelty and its crucial role in carboxysome function. While the catalytic and C-terminal domains of this protein bore resemblance to those in other  $\beta$ -type carbonic anhydrases, the N-terminal of CsoSCA was determined to be unique. By altering the structure of this enzyme by removing M1-R50 of the N-terminal domain, the necessity and function of this novel domain was analyzed.

A DNA construct was successfully designed and generated to delete these amino acids. The fragment was then inserted into a TOPO cloning vector. The TOPO plasmid was used to transform chemically competent Top 10 cells which allowed for electroporation of *E. coli* DY330 and homologous recombination of the construct into a portion of *H. neapolitanus* DNA (pTncsoS2::csoS3 in pT7-6 vector). This lengthened the homology on both the 5'-end and 3'-end of the designed construct. This lengthened, recombined plasmid DNA was successfully incorporated by in vivo recombination into the *H. neapolitanus* genome, generating two mutants.

To analyze the phenotype of the mutants resulting from the knocking out of amino acids 1-50 of the N-terminal domain of CsoSCA, growth rates of *H. neapolitanus* wildtype, the *csoS3* deletion mutant, and the *csoS3* truncation mutant were compared. The growth of each was monitored in air and CO<sub>2</sub> enriched air environments. CsoSCA dehydrates intracellular bicarbonate, equilibrating it to CO<sub>2</sub> to provide RuBisCO with its substrate. For the cell types grown in CO<sub>2</sub> enriched air (**Figure 22**), RuBisCO is in an environment that provides it with its substrate. Each cell type grows at approximately the

same rate. However, when the cell types are grown in air, the function of CsoSCA is more important. In **Figure 21**, the effects on CsoSCA function by gene alteration and deletion are evident. It can be seen that the wildtype grows at the greatest rate in air. The deletion mutant grows at a substantially decreased rate in air, indicating that the phenotype is greatly affected by the complete deletion of the *csoS3* gene. The truncated mutant grows at a decreased rate compared to the wild type but grows much better than the deletion mutant in air. Analyzing these results shows that deleting the first fifty amino acids of the N-terminal does affect the growth however not as substantially as deleting the *csoS3* gene entirely. A speculative hypothesis for the function of the N-terminal domain is that it is involved with targeting it to contact RuBisCO or other shell proteins of the carboxysome. The results of this experiment would support this. By removing a portion of the N-terminal domain, this domain's function is altered. If the N-terminal domain of CsoSCA can no longer function as effectively to target CsoSCA to these proteins, growth of the bacteria would be inhibited because CsoSCA may not be able to provide RuBisCO with its substrate as efficiently.

Further research could be done to measure the enzymatic activity of the mutant made. By following the progress of hydration of carbon dioxide and of dehydration of bicarbonate using stopped-flow spectrophotometry and changing pH indicators, enzyme kinetics could be observed. The mutant could also be tested for its ability to produce functional carboxysomes. Would the carboxysomes made by this mutant function, or would they be compromised? Finally, the experimental approach used here could be applied to remove the entire N-terminal domain to fully assess its necessity and its effects on CsoSCA function.

***Literature Cited:***

1. Heinhorst, S., Williams, E. B., Cai, F., Murin, C. D., Shively, J. M. & Cannon, G. C. (2006). Characterization of the carboxysomal carbonic anhydrase CsoSCA from *Halothiobacillus neapolitanus*. *J. Bacteriol.* 188: 8087-8094.
  
2. Cannon, G. C., Heinhorst, S., & Kerfeld, C. A. (2010). Carboxysomal carbonic anhydrases: Structure and role in microbial CO<sub>2</sub> fixation. *BBA - Proteins & Proteomics*, 1804(2): 382-392.
  
3. Sawaya, M.R., Cannon, G.C., Heinhorst, S., Tanaka, S., Williams, E.B., Yeates, T.O. & Kerfeld, C.A. (2006). The structure of beta-carbonic anhydrase from the carboxysomal shell reveals a distinct subclass with one active site for the price of two. *J Biol Chem*, 281: 7546–7555.
  
4. Valdebenito-Rolack, E. H., Araya, T. C., Abarzua, L. E., Ruiz-Tagle, N. M., Sossa, K. E., Aroca, G. E., & Urrutia, H. E. (2011). Thiosulphate oxidation by *Thiobacillus thioparus* and *Halothiobacillus neapolitanus* strains isolated from the petrochemical industry. *Electronic Journal of Biotechnology*, 14: 1-9.
  
5. Menon, B. B., Dou, Z., Heinhorst, S., Shively, J. M., & Cannon, G. C. (2008). *Halothiobacillus neapolitanus* carboxysomes sequester heterologous and chimeric RubisCO species. *Plos ONE*, 3(10), 1-10.

6. Cannon, G. C., Bradburne, C. E., Aldrich, H. C., Baker, S. H., Heinhorst, S., & Shively, J. M. (2001). Microcompartments in prokaryotes: carboxysomes and related polyhedra. *Applied and Environmental Microbiology*, 67(12): 5351-5361.
7. Dou, Z., Heinhorst, S., Williams, E. B., Murin, C. D., Shively, J. M., & Cannon, G. C. (2008). CO<sub>2</sub> fixation kinetics of *Halothiobacillus neapolitanus* mutant carboxysomes lacking carbonic anhydrase suggest the shell acts as a diffusional barrier for CO<sub>2</sub>. *The Journal of Biological Chemistry*, 283: 10377-10384.
8. Yu, D., Ellis, H. M., Lee, E., Jenkins, N. A., Copeland, N. G., & Court, D. L. (2000). An efficient recombination system for chromosome engineering in *Escherichia coli*. *Proc. Natl. Acad. Sci.*, 97(11): 5978-5983.
9. English, R. S., Jin, S., & Shively, J. M. (1995). Use of electroporation to generate a *Thiobacillus neapolitanus* carboxysome mutant. *Applied and Environmental Microbiology*, 61 (9): 3256-3260.